

## Threshold behavior in kinetic electron emission from oxide insulators

Han Kook Kim, Tae Seung Kim, and Jihwa Lee\*

*School of Chemical and Biological Engineering, Seoul National University, Seoul 151-744, South Korea*

Sam K. Jo

*Department of Chemistry, Kyung Won University, Sungnam, Kyungki 461-701, South Korea*

(Received 14 November 2006; revised manuscript received 9 August 2007; published 26 October 2007)

We have measured the yields  $\gamma$  of the secondary electrons emitted from MgO, BaO, and SiO<sub>2</sub> surfaces by impact of slow noble gas ions and identified the apparent threshold ion energies ( $E_0$ ) of kinetic electron emission from the discontinuity points in the  $\gamma$ - $E$  curves. We found that the center-of-mass threshold energy ( $E_{th}$ ) in the binary collision with an oxygen anion is projectile independent and equal to the sum of the band-gap energy and the electron affinity. Based on this threshold behavior, we propose that kinetic emission from oxide insulators occurs by direct collisional excitation of O  $2p$  electron to a continuum state via repulsive interactions with the electrons of a projectile.

DOI: [10.1103/PhysRevB.76.165434](https://doi.org/10.1103/PhysRevB.76.165434)

PACS number(s): 79.20.Rf, 47.55.dr, 61.80.Jh, 34.50.-s

### I. INTRODUCTION

Secondary electron emission from solid surfaces induced by slow ion impact has been ascribed to two different mechanisms: potential emission (PE)<sup>1</sup> and kinetic emission (KE).<sup>2</sup> PE results from ion neutralization by Auger-type electronic transitions involving two valence electrons in solids and proceeds spontaneously at any ion energy as long as the energetic requirement for the Auger process is satisfied, i.e.,  $IP \geq 2(E_g + \chi)$ , where IP is the ionization potential of the projectile,  $E_g$  the band-gap energy, and  $\chi$  the electron affinity. On the other hand, KE occurs by kinetic energy transfer to the target electrons, which is possible only above a certain threshold kinetic energy of a projectile. The mechanisms of KE in metals have now been fairly well established by extensive theoretical as well as experimental investigations.<sup>2,3</sup> Above the projectile velocity of  $1.75 \times 10^7$  cm/s (energy of  $\sim 300$  eV/amu),<sup>4</sup> incident ions can transfer enough energy to the free electrons in metals to eject them into the vacuum. KE by electron promotion to quasimolecular autoionizing states<sup>5,6</sup> and that by the excitation of shallow-lying core electrons followed by Auger transitions<sup>7</sup> have also been observed.

Ion-induced electron emission from insulator samples at low ion energies has also been extensively investigated, in particular, for MgO because of the important role it played in plasma display panels,<sup>8</sup> but these studies are mainly concerned with PE. On the contrary, KE has been much less studied, and its mechanism in insulators is still poorly understood. The momentum transfer mechanism valid for free electrons in metals is certainly not appropriate for KE from insulators because the valence electrons are localized around the anions. Riccardi *et al.*<sup>9</sup> have proposed that KE from the (111)-textured polycrystalline MgO surface occurs by collisional promotion of O  $2p$  electrons to the bulk exciton state, which decays to a continuum state due to the negative electron affinity of MgO(111).<sup>10</sup> However, this mechanism is not generally applicable to ordinary insulators with a positive electron affinity because the exciton state cannot couple to the continuum state. Vogan and Champion have observed

both electron and O<sup>-</sup> ion emission from oxygen-adsorbed Si(100)<sup>11</sup> and Mg(0001)<sup>12</sup> surface induced by low-energy ion impact, which they attributed to collision-induced electronic excitation to the (SiO<sub>x</sub><sup>-</sup>)<sup>\*</sup> and (MgO<sup>-</sup>)<sup>\*</sup> antibonding states followed by decay to result in the emission of O<sup>-</sup> ions or electrons. As described below in more detail, the surface atomic and consequently the electronic structures of O-adsorbed Mg are quite different from those of MgO, and therefore this mechanism cannot be applied to KE from MgO either.

In this paper, we present the energy dependence of the secondary electron emission yields  $\gamma$  of MgO, BaO, and SiO<sub>2</sub> surfaces measured with slow noble gas ions at energies of 20–120 eV, which shows well-defined threshold energies for KE. We found that for a given oxide, the apparent threshold energy ( $E_0$ ) increases with the projectile mass but the center-of-mass threshold energy ( $E_{th}$ ) in the binary collision with the oxygen anion is independent of the projectile mass. Furthermore,  $E_{th}$  is the same for different projectiles and equal to the sum of the band-gap energy and the electron affinity. On the basis of this threshold behavior, we propose that the KE from oxide insulators occurs by direct collisional excitation of an O  $2p$  electron to a continuum state via repulsive interactions with the electrons of a projectile.

### II. EXPERIMENT

The experimental system used for the present study will be described in detail elsewhere.<sup>13</sup> Briefly, it consists of an ion beam chamber and a UHV sample chamber. The UHV system is equipped with several evaporation cells, a quartz crystal microbalance, and provisions for Auger electron spectroscopy (AES) and ion scattering spectroscopy (ISS). MgO films (100 Å) were deposited on *n*-type Si(100) wafers at room temperature by reactive evaporation of Mg under an O<sub>2</sub> pressure of  $\sim 10^{-6}$  Torr. The Auger spectra showed a feature only at 32 eV, indicating that the film contains no metallic Mg.<sup>14</sup> BaO films (100 Å) were deposited by thermal evaporation of BaO on Si(100) substrates at 700 K. SiO<sub>2</sub> films (100 Å) grown on Si(100) by a standard dry oxidation

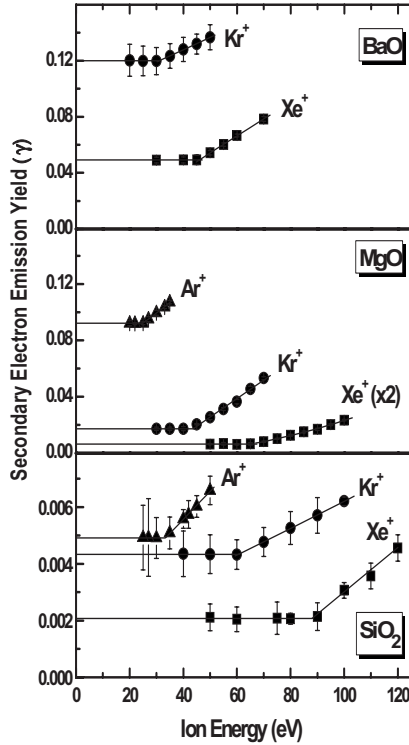


FIG. 1. The secondary electron emission yields  $\gamma$  of BaO, MgO, and SiO<sub>2</sub> as a function of ion energies for Ar<sup>+</sup>, Kr<sup>+</sup>, and Xe<sup>+</sup> at normal incidence.

process were also used for comparison. In all cases, Auger and ion scattering spectra showed contaminant-free oxide samples. The  $\gamma$  measurements were carried out using pulsed and mass-selected noble gas ion beams at normal incidence. Pulsing of dc ion beams was achieved by applying high voltage square-wave pulses of 5  $\mu$ s duration to the deflection plates at 50 Hz. A low-duty factor of  $<10^{-3}$  was essential for the measurements of the  $\gamma$ 's of the insulator samples in order to maintain surface charging negligible. The primary ion beam and the secondary electron currents were monitored with a Faraday cage and a skimmer-type collector, respectively. A positive bias of 5–20 V depending on the beam energy was applied to the collector with respect to the grounded substrate to ensure the collection of all the secondary electrons. The current pulse output was integrated and averaged using a charge-sensitive preamplifier and a gated integrator.

### III. RESULTS AND DISCUSSION

The measured  $\gamma$  values of MgO, BaO, and SiO<sub>2</sub> are shown in Fig. 1 for low-energy Ar<sup>+</sup>, Kr<sup>+</sup>, and Xe<sup>+</sup> ions at normal incidence. In all cases, the  $\gamma$  value is constant at low ion energies and increases almost linearly above a certain threshold energy. We attribute these two regimes to electron emission by PE and by KE, respectively. Since the two electron emission processes occur independently, the energy dependence of the total yield can be expressed as  $\gamma(E) = \gamma_{PE} + \gamma_{KE}(E)$ . The  $\gamma_{PE}$  increases in the order of SiO<sub>2</sub> < MgO < BaO for a given projectile and in the order of

TABLE I. The bulk (surface) band-gap energies ( $E_g$ ) and electron affinities ( $\chi$ ) of BaO, MgO, and SiO<sub>2</sub> in eV unit.  $E_{th}$  is the experimentally determined threshold for the center-of-mass energy ( $E_{c.m.}$ ) for the kinetic secondary electron emission (KE).

Oxides	$E_g$	$\chi$	$E_g + \chi$	$E_{th}$
MgO	7.8 <sup>a</sup> (6.35) <sup>b</sup>	0.85 <sup>c</sup>	8.65 (7.0)	7.2 $\pm$ 0.3
BaO <sup>d</sup>	3.7	1.3–1.5	5–5.2	5.0 $\pm$ 0.3
SiO <sub>2</sub>	9.0 <sup>e</sup>	0.9 <sup>f</sup>	9.9	9.8 $\pm$ 0.5

<sup>a</sup>Reference 15.

<sup>b</sup>Reference 16.

<sup>c</sup>Reference 17.

<sup>d</sup>Reference 18.

<sup>e</sup>Reference 19.

<sup>f</sup>Reference 20.

Xe<sup>+</sup> < Kr<sup>+</sup> < Ar<sup>+</sup> for a given oxide. These trends can be qualitatively understood on the basis of the energetics of PE and the band parameters listed in Table I below.

We note in Fig. 1 that the apparent threshold energies ( $E_0$ ) are by far smaller than the KE threshold for free electrons in metals. For example,  $E_0 \sim 25$  eV for Ar<sup>+</sup>/MgO, whereas  $E_0 \sim 400$  eV for Ar<sup>+</sup>/gold.<sup>5</sup> Furthermore, the increase in  $\gamma_{KE}$  with the projectile energy is also much greater than that for metal samples.<sup>3,5</sup> These observations suggest that the large  $\gamma_{KE}$  as well as the small  $E_0$  value in KE from insulator surfaces are related to the localized character of their valence electrons. Since the  $\gamma$ - $E$  curves measured with He<sup>+</sup> and Ne<sup>+</sup> ions showed no discontinuity down to the ion energy of 20 eV, those data are not presented here. In the case of BaO, the absolute  $\gamma$  values varied as much as  $\sim 50\%$ , depending on the O<sub>2</sub> partial pressure during deposition and on the annealing temperature. Thus, the BaO film for which the  $\gamma$  data are presented in Fig. 2 may not have a stoichiometric surface composition. Nevertheless, the threshold ion energy of KE did not change significantly.

From the observation that  $\gamma_{KE}$  increases linearly with ion energy above the apparent threshold energy ( $E_0$ ), the data points above  $E_0$  were least-squares fitted as shown by the solid lines in Fig. 1. Each  $E_0$  value was determined from the intersecting point of the two straight lines below and above  $E_0$ . For a given oxide,  $E_0$  increases with the projectile mass. Since collision is a relative motion between a projectile ( $m_1$ ) and a target ion ( $m_2$ ), the collision energy ( $E_{c.m.}$ ) in the center-of-mass frame is the relevant energy in KE.  $E_{c.m.}$  in a binary head-on collision is related to the kinetic energy ( $E$ ) of the projectile by

$$E_{c.m.} = \frac{1}{2} \mu v^2 = \frac{m_2}{m_1 + m_2} E, \quad (1)$$

where  $v$  is the velocity and  $\mu$  the reduced mass. The  $\gamma$  data in Fig. 1 are replotted in Fig. 2 as a function of the  $E_{c.m.}$  values calculated with Eq. (1) using  $m_2 = 16$ , the mass of oxygen. Here, one can clearly see that for a given oxide, the onset of KE starts at the same  $E_{c.m.}$  for the different projectiles as indicated by the dashed vertical lines. The projectile dependence of  $E_0$  is shown in Fig. 3, where  $E_0$  is plotted

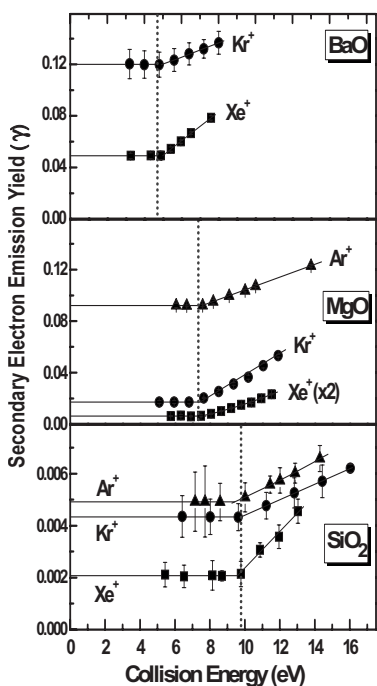


FIG. 2. The  $\gamma$  vs  $E$  replotted against the center-of-mass collision energy ( $E_{c.m.}$ ) of the projectile-oxygen binary collision from the data in Fig. 1. The threshold ion energies ( $E_{th}$ ) of kinetic emission are indicated by the vertical dashed lines.

against the mass ratio  $m_1(\text{projectile})/m_2(\text{O})$ . From both the intercept and the slope of the linear plot, we can determine the  $E_{th}$  for each oxide. The  $E_{th}$  values thus obtained are  $5.0 \pm 0.3$ ,  $7.2 \pm 0.3$ , and  $9.8 \pm 0.5$  eV for BaO, MgO, and SiO<sub>2</sub>, respectively. Though there is no *a priori* physical basis to assume a linear increase in  $\gamma_{KE}$  with the projectile energy, a quite linear energy dependence was observed up to the ion energy of  $\sim 200$  eV. The linear extrapolation may introduce some error in  $E_0$ , but the error in  $E_{th}$  should be small because of the relation  $E_{th} = [m_2 / (m_1 + m_2)] E_0$ , which is  $\sim 0.1$  for Xe<sup>+</sup>.

The center-of-mass threshold energies ( $E_{th}$ ) determined experimentally are listed in Table I together with the band

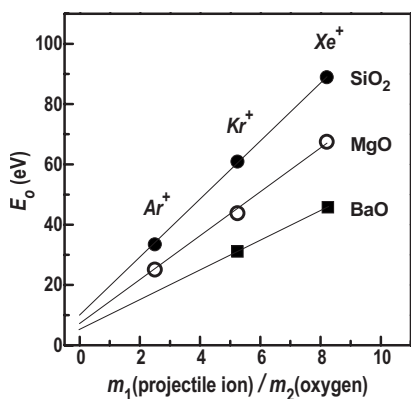


FIG. 3. The apparent threshold ion energy ( $E_0$ ) of kinetic emission plotted against the mass ratio  $m_1/m_2$ . From the relation  $E_0 = (1 + m_1/m_2) E_{th}$ , the center-of-mass threshold energy ( $E_{th}$ ) values, obtained from the slope and the intercept of the linear plots, are also shown.

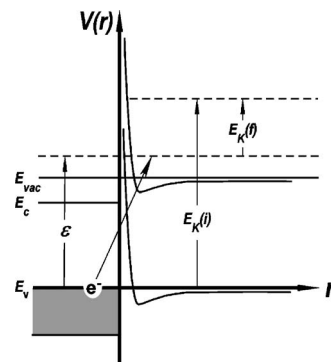


FIG. 4. A schematic energy diagram for kinetic secondary electron emission from oxide surfaces. An electron is directly excited to the continuum state by kinetic energy transfer.  $E_k(i)$  and  $E_k(f)$  represent the initial and final collision energies, respectively, and  $\epsilon$  the electron excitation energy.

parameters of the oxides reported in the literature.<sup>15–20</sup> Interestingly,  $E_{th}$  coincides with the sum  $E_g + \chi$  within the experimental uncertainty. This implies that KE occurs when the  $E_{c.m.}$  exceeds the minimum energy required to eject an electron from valence band of an oxide. In the case of MgO, the  $E_{th}$  value agrees better with the sum of  $\chi$  and the surface  $E_g$ , which is smaller by  $\sim 1.5$  eV than the bulk value.<sup>16</sup> This may also be the case for BaO and SiO<sub>2</sub>, considering the fact that the  $\chi$  and surface  $E_g$  values of oxide materials are not precisely known and that they also depend on the crystallographic surface orientation.<sup>10</sup>

The observation that  $E_{th}$  is equal to  $E_g + \chi$  immediately leads us to propose that KE from oxide insulators occurs by collision-induced direct single-electron excitation to a continuum state. If it had occurred by an indirect process involving an intermediate electronic state or by a multielectron excitation process, the  $E_{th}$  larger than  $E_g + \chi$  would have been measured. The process of KE can be envisioned as follows (refer to Fig. 4). An incident ion, which is first neutralized either by Auger process or by resonant tunneling in front of an O<sup>2-</sup> anion, continues to move forward to penetrate the electron cloud of the O<sup>2-</sup> anion until it turns around at the classical turning point. During the close collision, the energy of O 2p electron is continuously raised with the decreasing internuclear distance due to the repulsive interactions with the projectile electrons. If the perturbed O 2p level falls within the band gap of the oxide, the electron reverts to its initial state as the collision partners separate adiabatically without any energy transfer to a target electron. On the other hand, if it lies above the vacuum level ( $E_{vac}$ ), the perturbed state can evolve directly into a continuum state, resulting in the emission of an electron. Similarly, the band-gap excitation by kinetic energy transfer would set in when the  $E_{c.m.}$  just exceeds  $E_g$ . In this case, the band-gap excitation threshold could be determined by measuring the surface conductivity as a function of the ion energy. Such measurements can provide one with the electron affinity of an insulator, which is difficult to obtain by other experimental methods.

Riccardi *et al.*<sup>9</sup> have measured the energy distributions of electrons emitted from a (111)-textured polycrystalline MgO film by Na<sup>+</sup> or noble gas ion impacts that were nearly inde-

pendent of the projectile type and of the energy below  $\sim 1$  keV. The results led them to propose that the O  $2p$  electron is excited to the bulk exciton state, which migrates to the surface and subsequently decays to a continuum state due to the negative  $\chi$  of MgO(111).<sup>10</sup> One may wonder why KE should occur only via the bulk exciton and not via the direct excitation to the continuum state as well. It will be interesting to measure the KE threshold energy of MgO(111) surface and compare it with that we report here.

Concurrent electron and O<sup>-</sup> ion emissions from O-adsorbed Si(100) (Ref. 9) and Mg(0001) (Ref. 10) surfaces by low-energy ion impact have been interpreted as resulting from electronic excitations to the (SiO<sub>x</sub>)<sup>\*</sup> and (MgO)<sup>\*</sup> antibonding states, respectively. We have also measured the  $\gamma$  of polycrystalline Mg films at room temperature with 250 eV He<sup>+</sup> ions as a function of O<sub>2</sub> exposures, reproducing the result of Vogan and Champion.<sup>11</sup> However, the measured  $\gamma$  value of  $\sim 0.50$  for the O-saturated Mg surface is by far smaller than 1.47 measured with our MgO sample. Moreover, ISS and AES measurements revealed that the O-adsorbed Mg surface has considerable O atom deficiency and is very thin due to the diffusion-limited oxide growth at room temperature. These results tell that the two samples have quite different atomic compositions and consequently different electronic structures. In the case of O-adsorbed Mg film, the loss of surface O atoms was clearly visible even during the acquisition of ISS spectra. Our MgO sample, however, suffered no noticeable surface compositional change even after bombardments of  $\sim 10^{16}$  He<sup>+</sup> ions/cm<sup>2</sup> at 500 eV, confirmed by ISS. The  $\gamma$  value measured after heating the samples to remove the surface charge was almost the same as that without ion bombardments, indicating that O<sup>-</sup> emission is negligible in our  $\gamma$  measurements. The O<sup>-</sup> ion left behind as a result of KE from the O<sup>2-</sup> ion is still bound because of the attractive, though weaker, Madelung potential, and therefore it cannot be emitted into the vacuum.

In calculating the  $E_{c.m.}$  with Eq. (1), it may be more reasonable to use a projectile-dependent effective target mass because of the finite size of the projectile. Considering the large atomic size of Xe, one may think that a Xe atom collides simultaneously with both an O<sup>2-</sup> ion and a neighboring cation on the oxide surfaces, in particular, on BaO surface with the large Ba<sup>+</sup> cations. Nevertheless, the  $E_{th}$  values obtained for Ar<sup>+</sup>, Kr<sup>+</sup>, and Xe<sup>+</sup> ions using the mass of oxygen were found to be identical for a given oxide. This implies that the collision that induces KE is similar to the one between a projectile and an isolated O<sup>2-</sup> ion. At near-threshold energies, only the collisions with very small impact parameters can transfer enough energy to cause KE and therefore even a Xe atom would not feel the mass of the neighboring cation.

#### IV. CONCLUSION

We have measured the yields  $\gamma$  of secondary electron emissions from MgO, BaO, and SiO<sub>2</sub> by slow noble gas ion bombardments and obtained the threshold energies of kinetic secondary electron emission from the discontinuity points in the  $\gamma$ - $E$  curves. The apparent threshold energy for a given oxide increases with the projectile mass, but the center-of-mass threshold energy in the binary collision with an oxygen anion is projectile independent. Furthermore, it is equal to the sum of the band-gap energy and the electron affinity of a given oxide. On the basis of our  $E_{th}$  data analyses, we propose that KE from oxide insulators occurs by direct collisional excitation of O  $2p$  electrons to the continuum states via repulsive interactions with the electrons of a projectile.

#### ACKNOWLEDGMENT

This work was supported by Samsung Display Industry through Samsung-Seoul National University Display Innovation Program (SSDIP).

\*Corresponding author; jihwalee@plaza.snu.ac.kr

<sup>1</sup>H. D. Hagstrum, Phys. Rev. **96**, 336 (1954); **122**, 83 (1961).

<sup>2</sup>D. Hasselkamp, in *Particle Induced Electron Emission II*, edited by G. Höhler, Springer Tracts in Modern Physics Vol. 123 (Springer-Verlag, Berlin, 1991), p. 1.

<sup>3</sup>R. Baragiola, in *Low Energy Ion-Surface Interactions*, edited by J. W. Rabalais (Wiley, New York, 1994), Chap. 4, p. 188, and references therein.

<sup>4</sup>E. V. Alonso, R. A. Baragiola, J. Ferron, M. M. Jakas, and A. Oliva-Florio, Phys. Rev. B **22**, 80 (1980).

<sup>5</sup>G. Lakits, F. Aumayr, M. Heim, and H. Winter, Phys. Rev. A **42**, 5780 (1990).

<sup>6</sup>A. Niehaus, Phys. Rep. **186**, 149 (1990).

<sup>7</sup>O. Grizzi, M. Shi, H. Bu, J. W. Rabalais, and R. A. Baragiola, Phys. Rev. B **41**, 4789 (1990).

<sup>8</sup>*Nanoelectronics and Information Technology*, edited by R. Waser (Wiley-VCH, Weinheim, 2003), Chap. 39, and references therein.

<sup>9</sup>P. Riccardi, M. Ishimoto, P. Barone, and R. A. Baragiola, Surf. Sci. **571**, L305 (2004); P. Riccardi, P. Barone, A. Bonanno, A.

Oliva, P. Vetro, M. Ishimoto, and R. A. Baragiola, Nucl. Instrum. Methods Phys. Res. B **230**, 455 (2005).

<sup>10</sup>V. E. Heirich and P. A. Cox, *The Surface Science of Metal Oxide* (Cambridge University Press, Cambridge, 1994), Chap. 4, p. 102.

<sup>11</sup>W. S. Vogan and R. L. Champion, Surf. Sci. **492**, 83 (2001).

<sup>12</sup>W. S. Vogan, R. L. Champion, and V. A. Esaulov, Surf. Sci. **538**, 211 (2003).

<sup>13</sup>Han Kook Kim, Deok Hyun Kim, II, Sin Choi, and Jihwa Lee (unpublished).

<sup>14</sup>M.-C. Wu, J. S. Corneille, J.-W. He, C. A. Estrada, and D. Wayne, J. Vac. Sci. Technol. A **10**, 1467 (1992).

<sup>15</sup>R. C. Whited, C. J. Flaten, and W. C. Walker, Solid State Commun. **13**, 1903 (1973).

<sup>16</sup>P. A. Cox and A. A. Williams, Surf. Sci. **175**, L782 (1986).

<sup>17</sup>K. Y. Tsou and E. B. Hensley, J. Appl. Phys. **45**, 47 (1974).

<sup>18</sup>H. B. DeVore and J. W. Dewdney, Phys. Rev. **83**, 805 (1951).

<sup>19</sup>R. E. Thomas, A. Shih, and G. A. Hass, Surf. Sci. **75**, 239 (1978).

<sup>20</sup>B. E. Deal, E. H. Snow, and C. A. Mead, J. Phys. Chem. Solids **27**, 1873 (1966).